Electronic Supplementary Material (ESI) for Journal of Materials Chemistry C.


# Supporting Information

# A Self-healing and Stretchable Light-emitting Device

*Xiang Shi, Xufeng Zhou, Ye Zhang, Xiaojie Xu, Zhitao Zhang,*

*Peng Liu, Yong Zuo, Huisheng Peng**

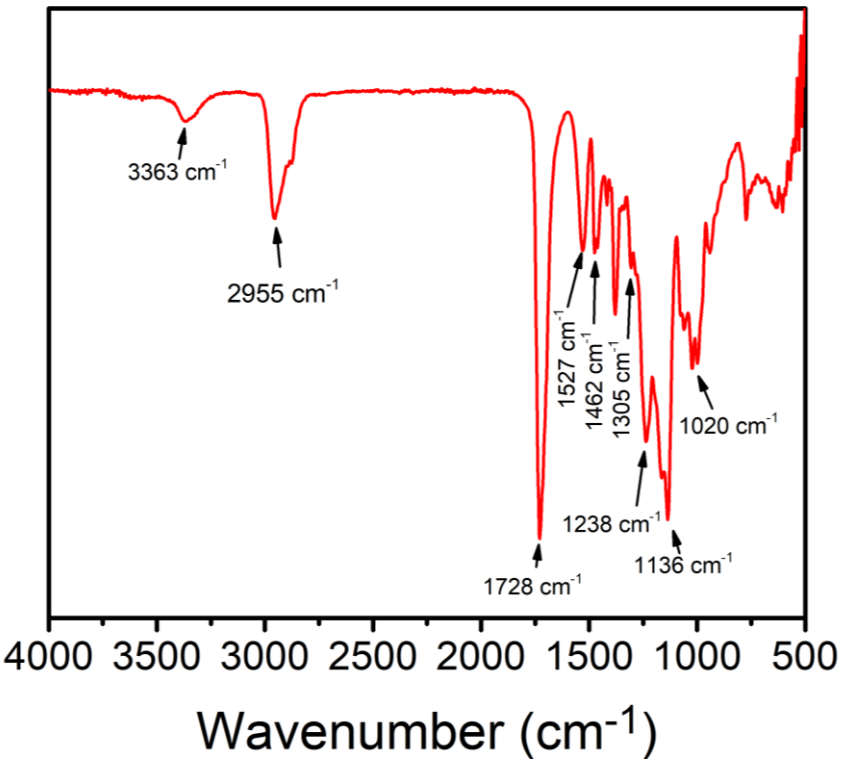


**Figure S1.** Fourier transform infrared spectrum of synthesized self-healing PU with the following characteristic peaks of 3363 $cm^{-1}$ (ν(-NH-)), 2955 $cm^{-1}$ (ν($CH_3$,$CH_2$)), 1728 $cm^{-1}$ (ν (C=O)), 1527 $cm^{-1}$ (δ(C-N-H)), 1462 $cm^{-1}$ (δ($CH_2$)), 1305 $cm^{-1}$ (δ(C(C=O)-N-H)), 1238 $cm^{-1}$, 1136 $cm^{-1}$ (ν(C-O-C)) and 1020 $cm^{-1}$ (δ(C-O-C)).

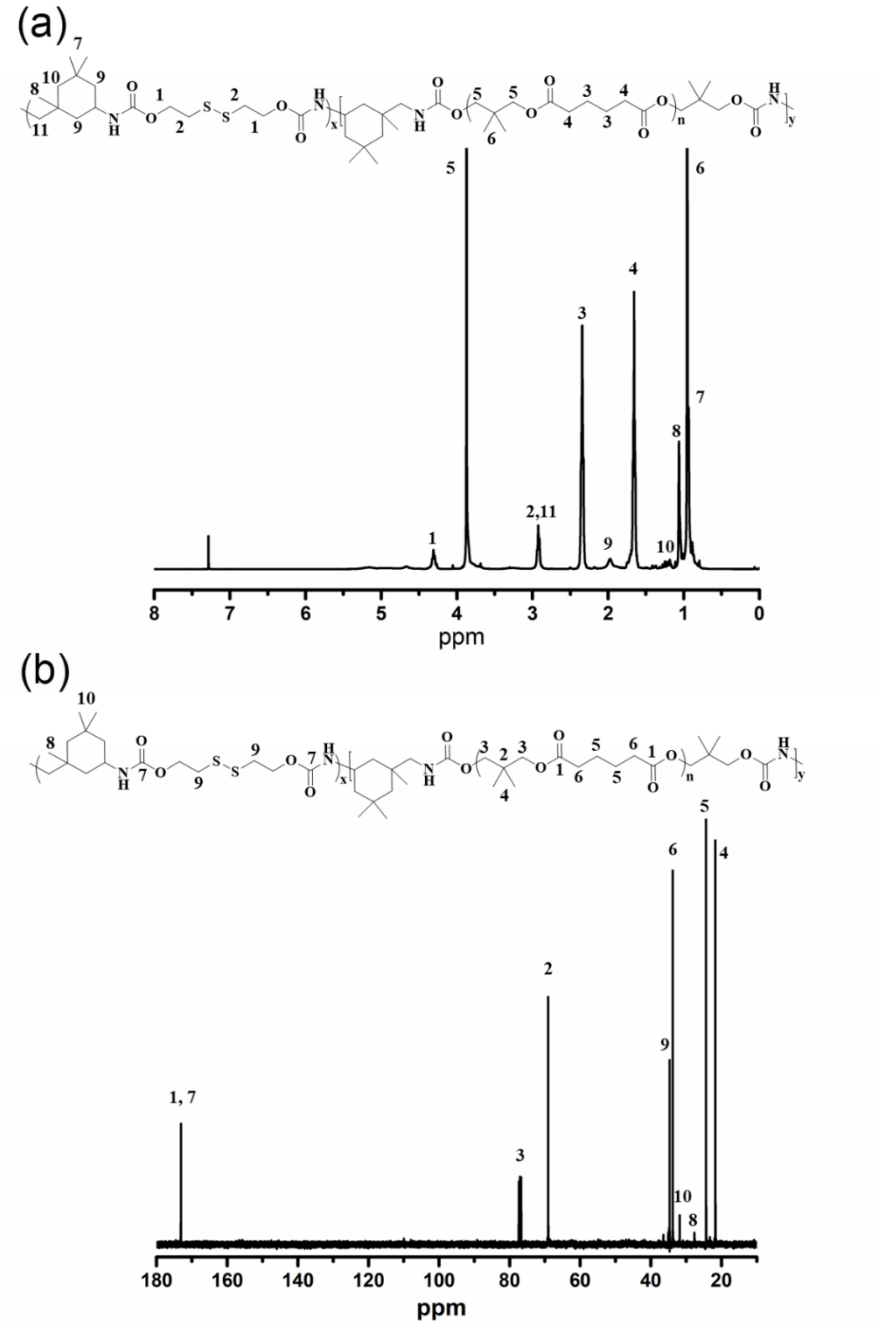


**Figure S2.** (a) $^{1}$H NMR spectrum ($CDCl_3$) of self-healing PU. δ (ppm) = 7.28 ($CDCl_3$), 4.32 (1H, -O-$CH_2$-), 3.88 (5H, -O-$CH_2$ of PNGA), 2.92 (2H, 11H, , S-$CH_2$-, -N-$CH_2$-), 2.35 (3H, -$CH_2$- of PNGA), 1.92 (9H, -$CH_2$- of IPDI), 1.66 (4H, O=C-$CH_2$- of PNGA), 1.20-1.17 (10H, -$CH_2$- of IPDI), 1.07 (8H, -$CH_3$ of IPDI), 1.050 (6H, –$CH_3$ of PNGA), and 0.94 (1H, -$CH_3$ of IPDI). (b) $^{13}$C NMR spectrum ($CDCl_3$) of self-healing PU. δ (ppm) = 173.0 (1C, 2C, C=O), 77.2 (3C, O-$CH_2$-), 69.0 (2C, $CH_2$-$C(CH_3)_2$-$CH_2$), 34.7 (9C, S-$CH_2$-), 33.8 (6C, $CH_2$), 31.8 (10C, $CH_3$), 27.6 (8C, $CH_3$), 24.3 (5C, $CH_2$), 21.7 (4C, $CH_3$).

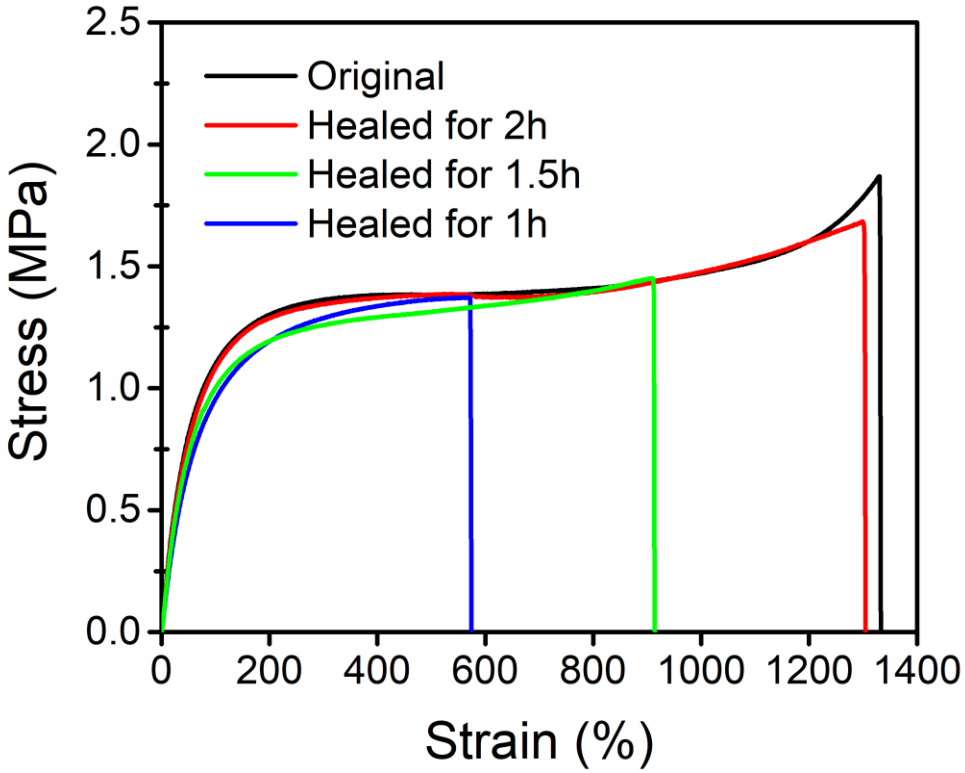


**Figure S3.** Tensile stress-strain curves of original and healed PU.

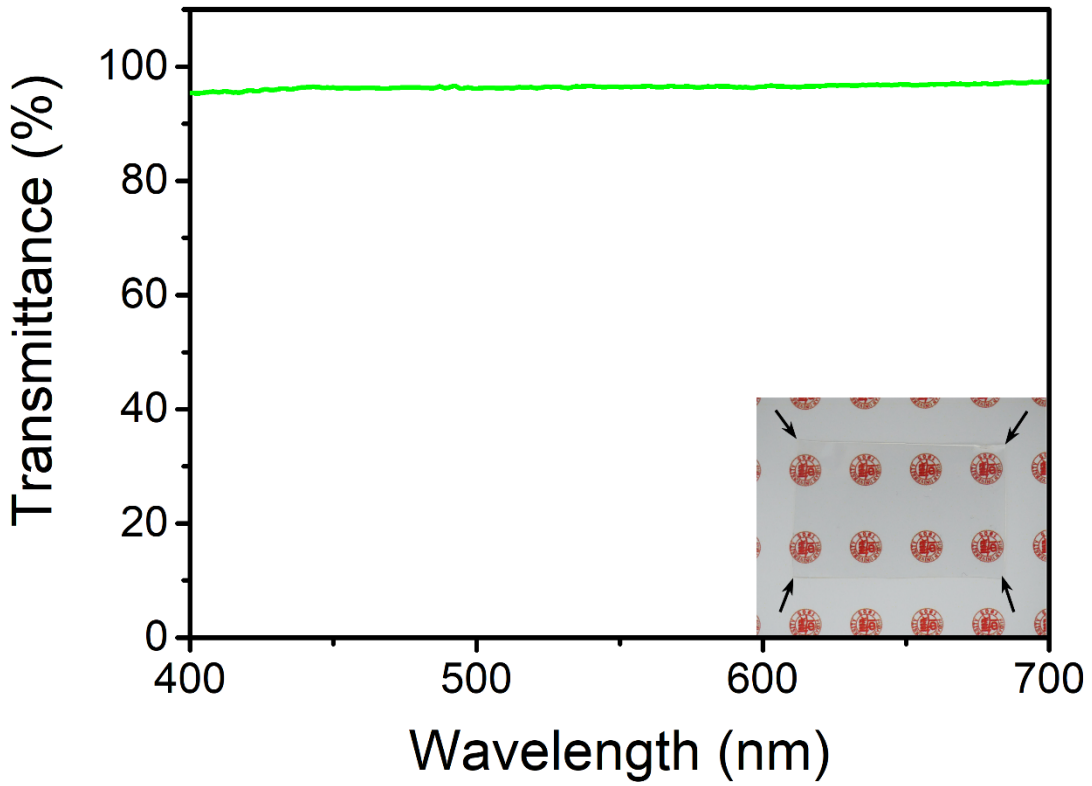


**Figure S4.** Dependence of optical transmittance on wavelength for a 200 μm-thick PU film (inset, photograph of a transparent PU film).

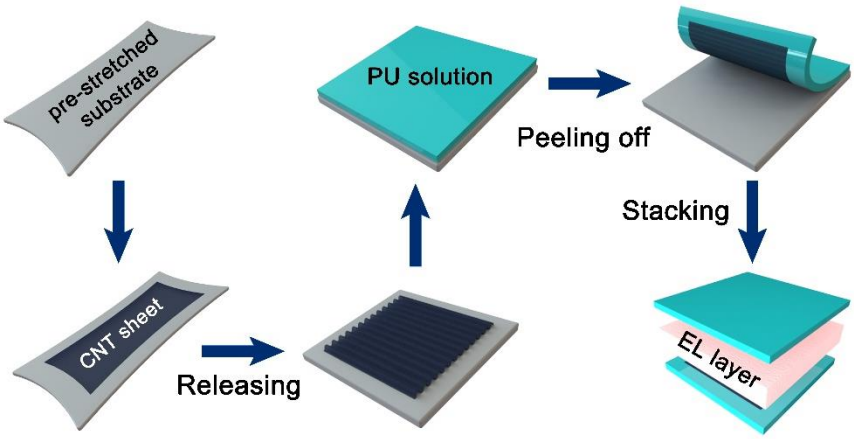


**Figure S5.** Schematic illustration to the fabrication process of a self-healing EL device.

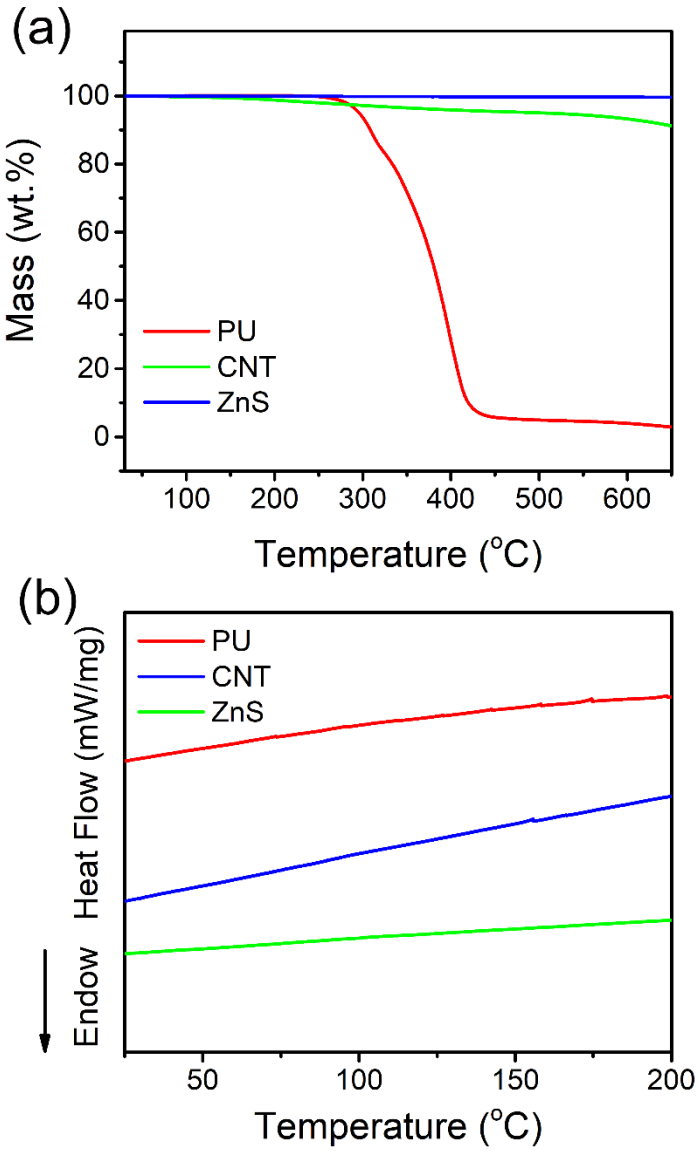


**Figure S6.** (a) Thermal gravimetric analysis (TGA) and (b) differential scanning calorimetry (DSC) of PU, ZnS phosphor and carbon nanotube.

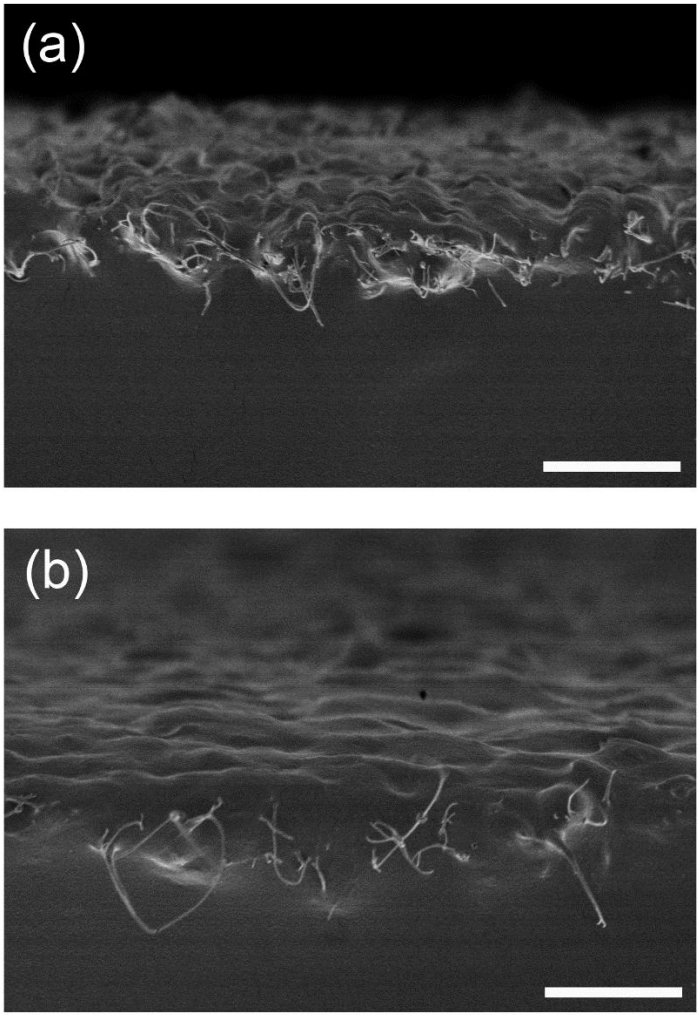


**Figure S7.** Cross-sectional SEM images of aligned CNT/PU composite electrodes with the interface being parallel (a) and vertical (b) to the alignment of CNTs. Scale bars, 2.5 μm.

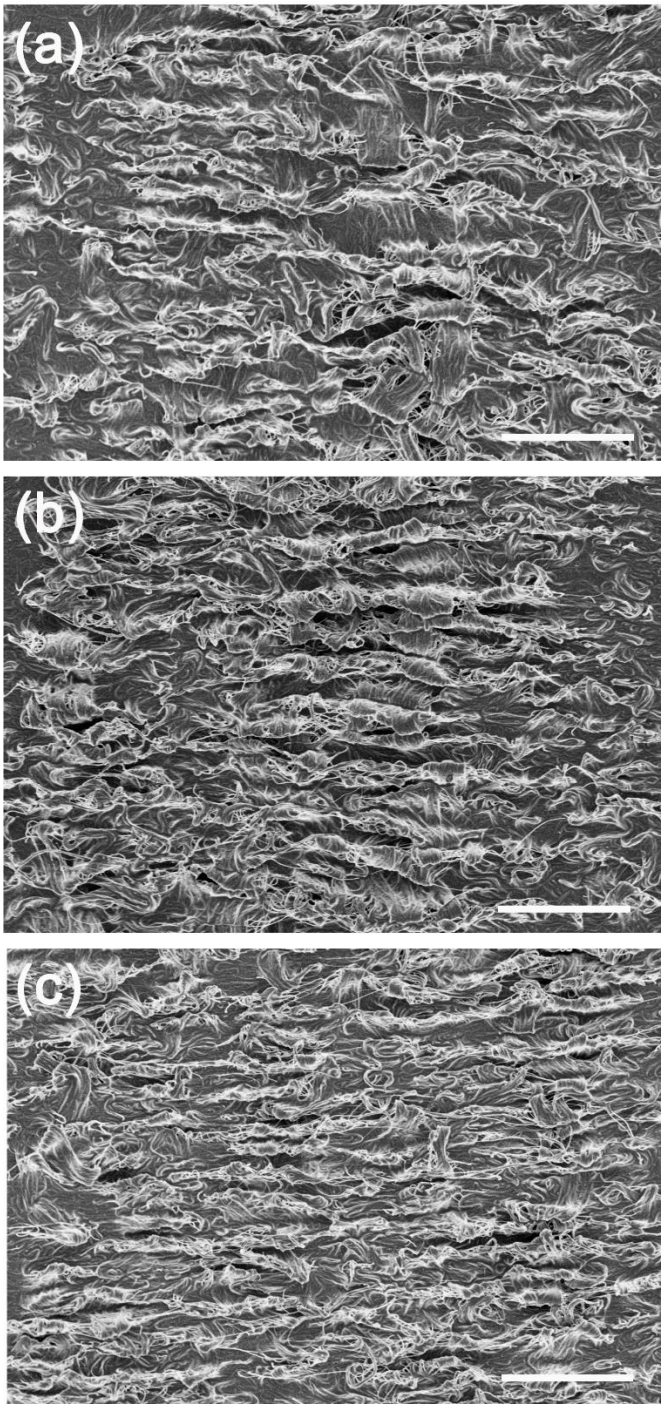


**Figure S8.** SEM images of bare wrinkled CNT sheets on the elastic films released from the pre-stretched substrates with the strains of (a) 200%, (b) 300% and (c) 400%. Scale bars, 5μm.

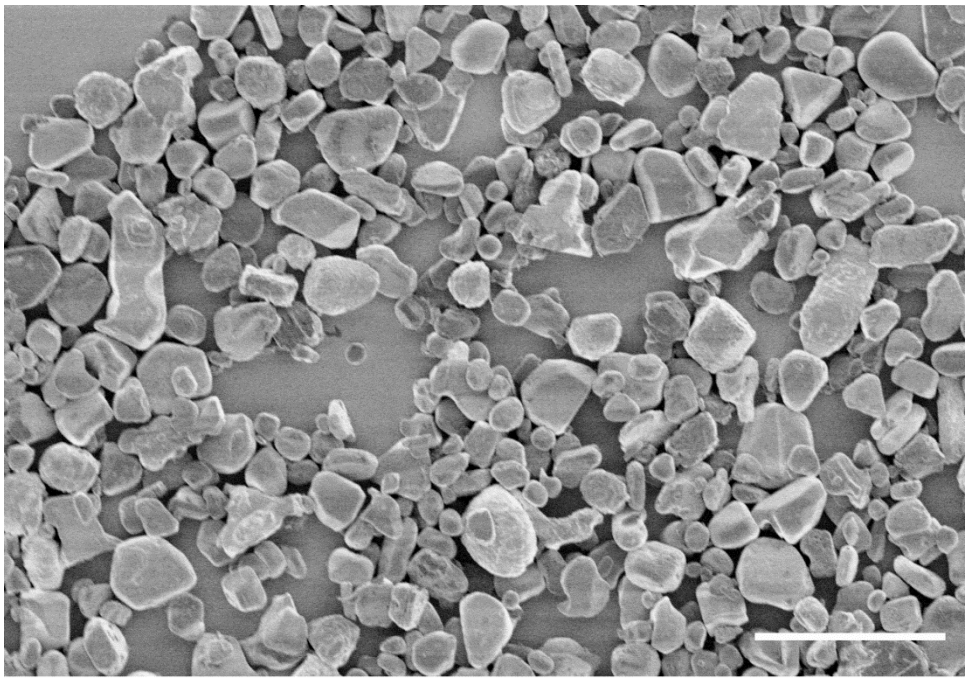

**Figure S9.** SEM image of ZnS phosphor. Scale bar, 50 μm.

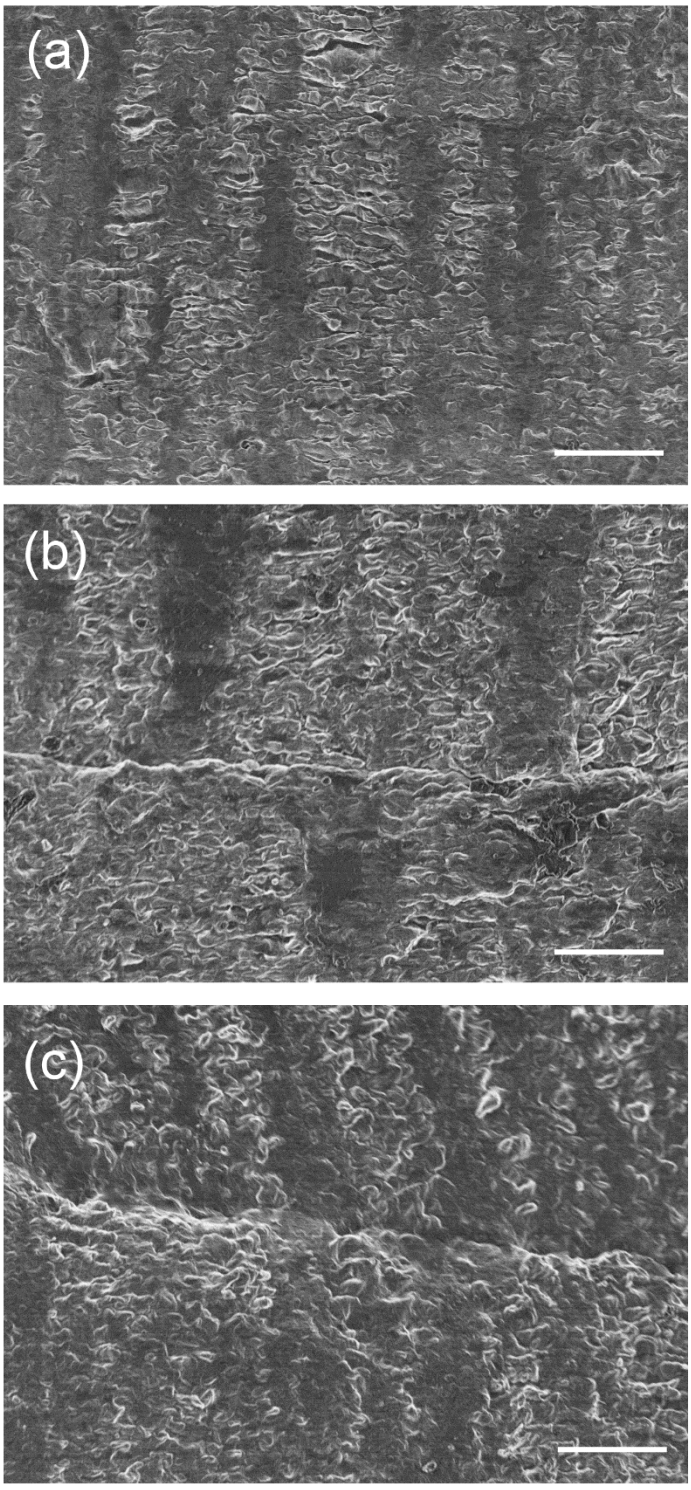


**Figure S10.** SEM images of the CNT/PU composite electrodes (a) before and (b) after healing and (c) stretched to 400%. Scale bars, 10 μm.

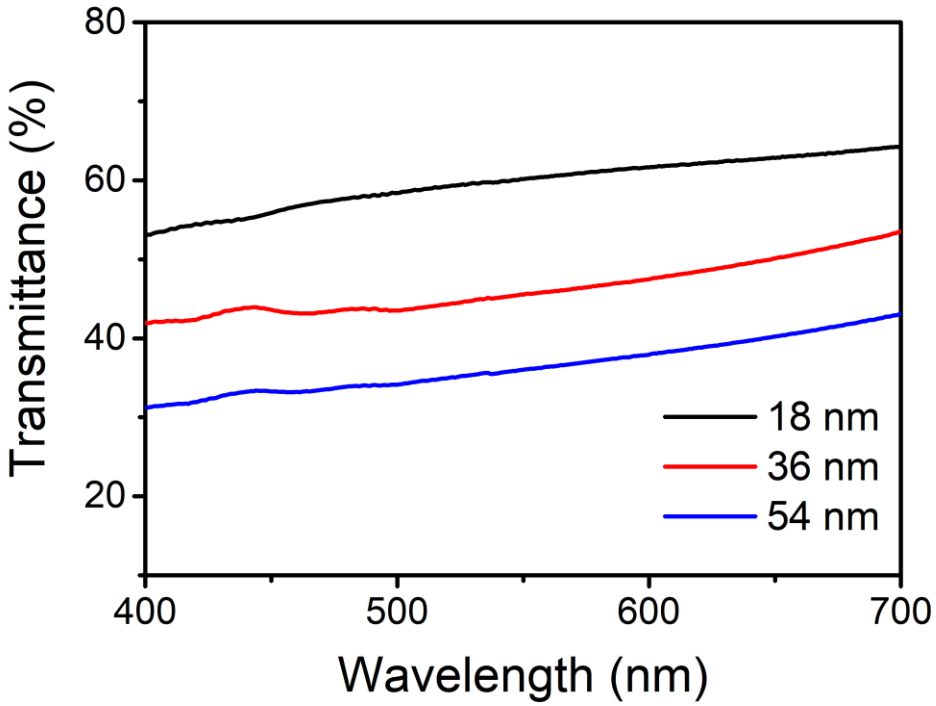


**Figure S11.** Dependence of optical transmittance on the thickness of aligned CNT sheet electrodes.

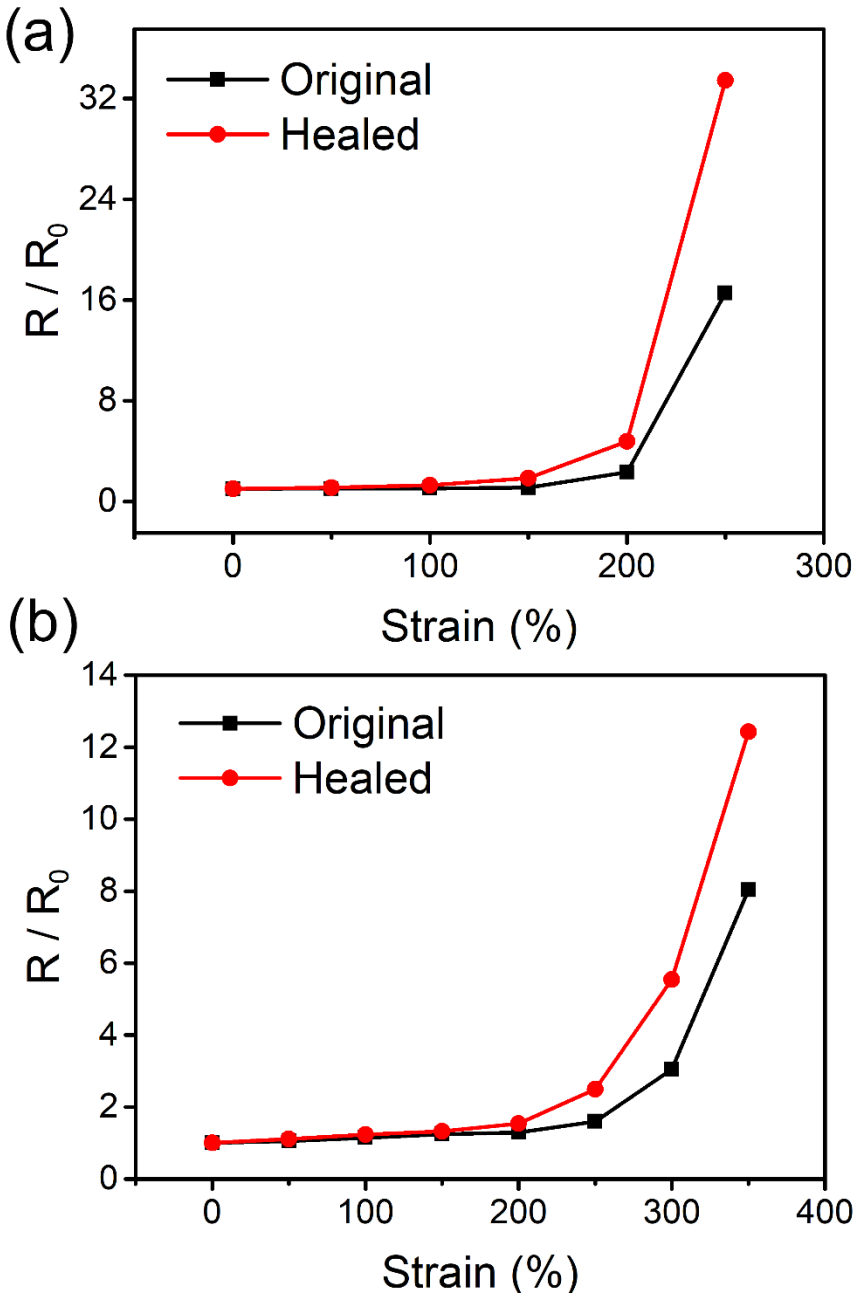


**Figure S12.** Dependence of electrical resistance on the pre-stretched strain of (a) 200% and (b) 300%.

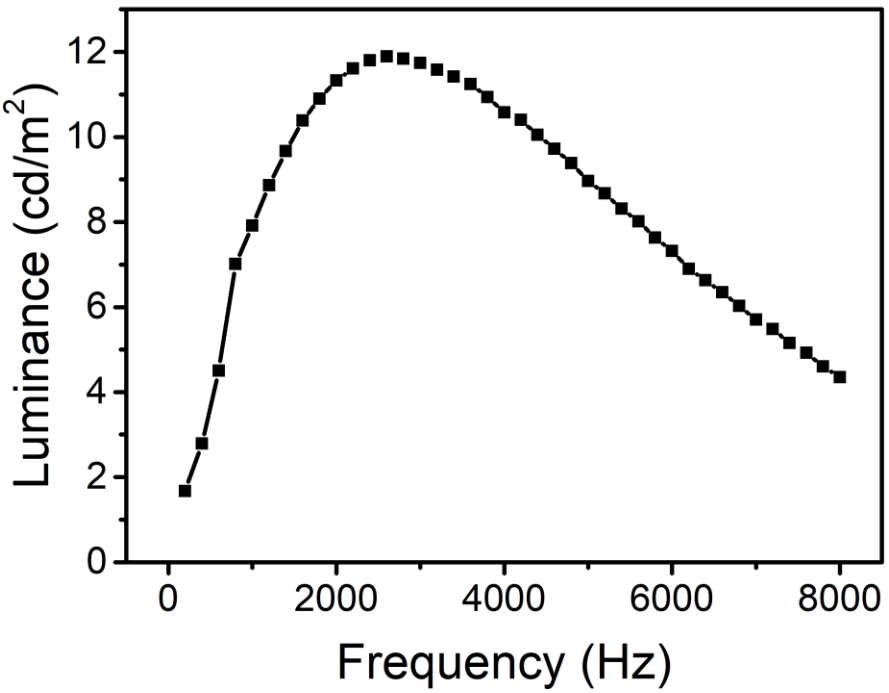


**Figure S13.** Dependence of luminance on the applied frequency.

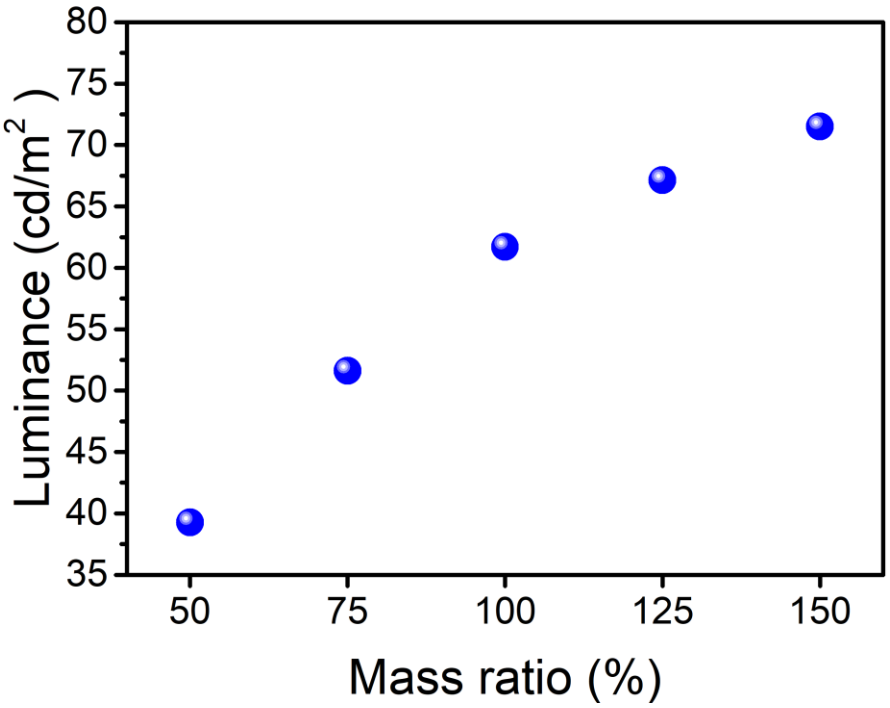


**Figure S14.** Dependence of luminance on the ZnS mass ratio (m(ZnS)/m(PU)) (driving voltage of 8 V/μm).

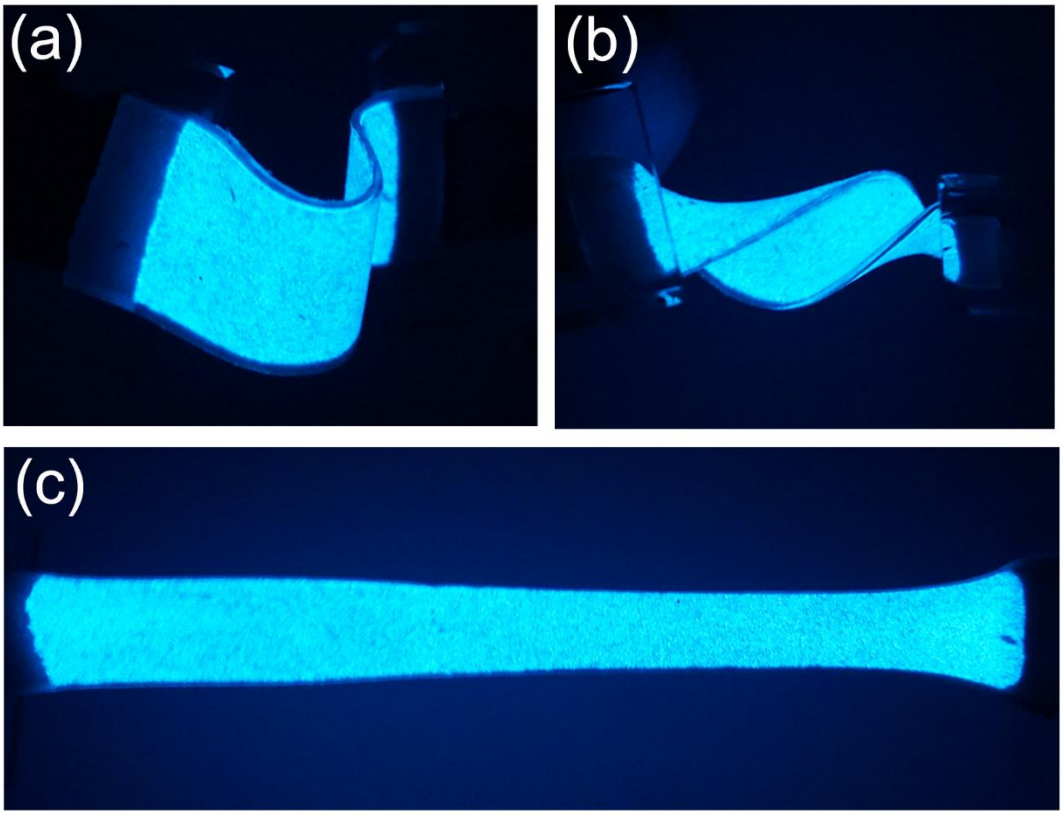


**Figure S15.** Photographs of a healed EL device being bent (a), twisted (b) and stretched (c).

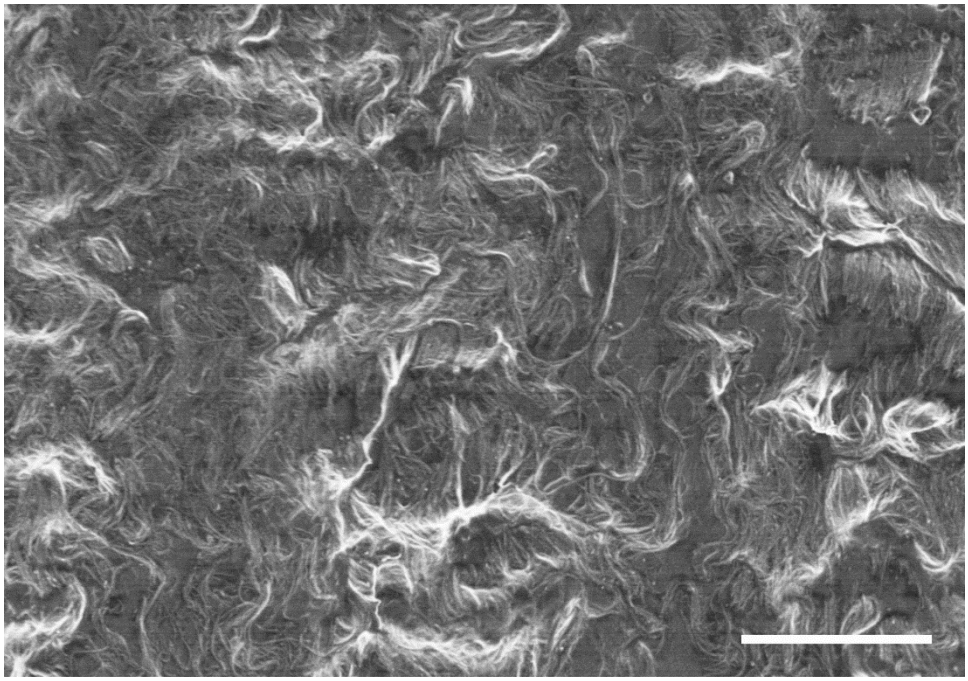

**Figure S16.** SEM image of a CNT/PU composite electrode at a strain of 400%. Scale bar, 5 μm.

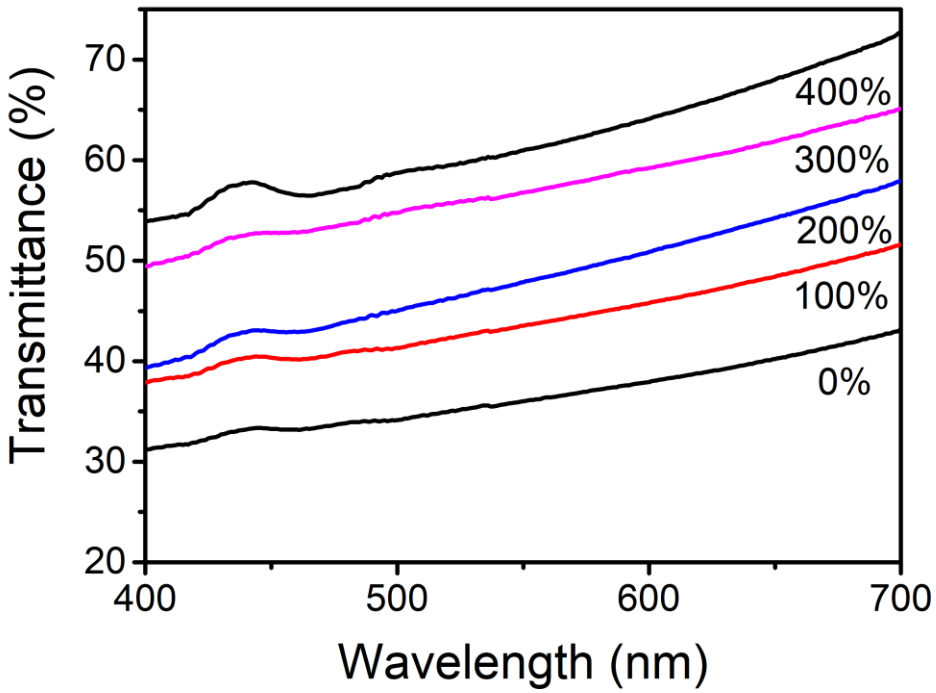


**Figure S17.** Dependence of optical transmittance on strain of aligned CNT sheets.

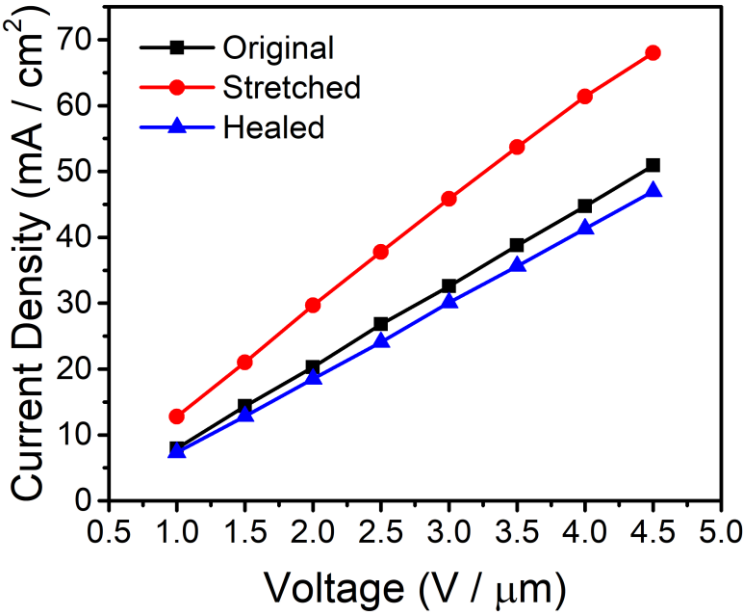


**Figure S18.** Current density-voltage curve of the EL device before and after healing and stretching.

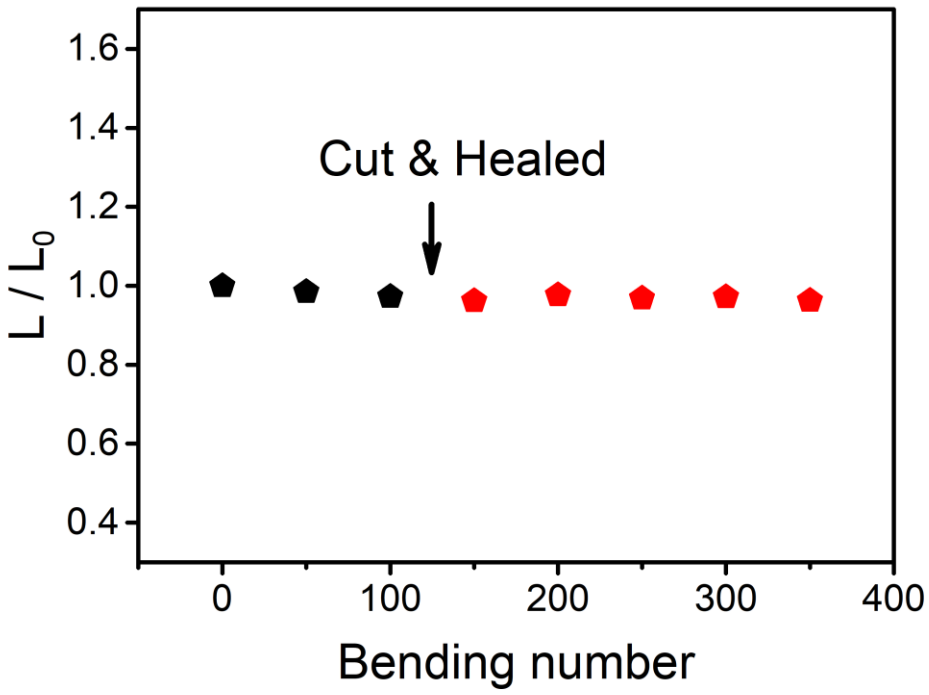


**Figure S19.** Dependence of luminance on the stretching cycle number. $L_0$ and L correspond to the luminance before and after bending, respectively.

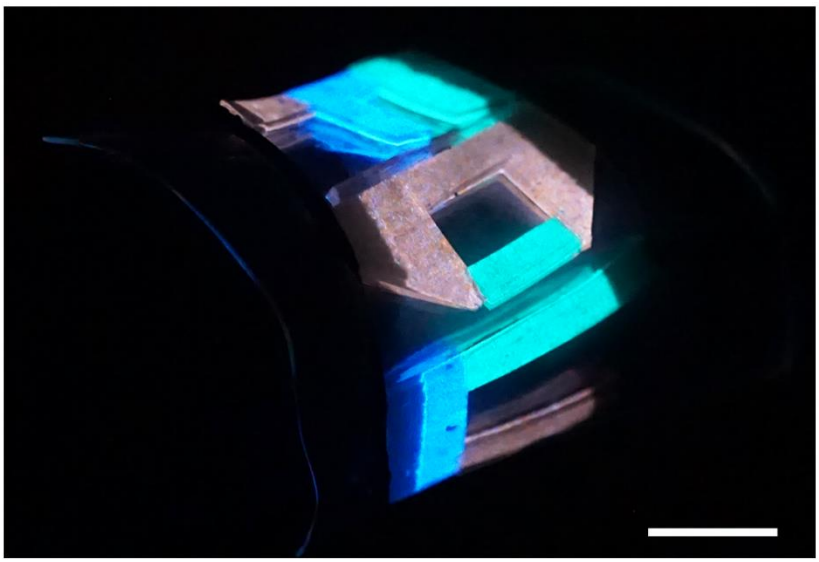

**Figure S20.** Flexible multi-colored device wrapped on a finger. Scale bar, 0.5 cm.